Journal of ELECTRONIC MATERIALS, Vol. 41, No. 11, 2012
DOI: 10.1007/s11664-012-2210-7


# Hydrothermal Synthesis and Electrochemical Performance of $MnCo_2O_4$ Nanoparticles as Anode Material in Lithium-Ion Batteries

HAOWEN LIU[1,2,3] and JIN WANG[1]

1.—Key Laboratory of Catalysis and Materials Science of the State Ethnic Affairs Commission & Ministry of Education, South-Central University for Nationalities, Wuhan 430074, Hubei Province, People's Republic of China. 2.—e-mail: liuhwchem@mail.scuec.edu.cn. 3.—e-mail: liuhw0526@hotmail.com

In this work, nanosized $MnCo_2O_4$ was prepared by the hydrothermal method. The crystalline phase, the morphology, and the valences of the elements in the obtained samples were characterized by x-ray diffraction (XRD), transmission electron microscopy (TEM), and x-ray photoelectron spectrometry (XPS), respectively. XRD showed that the prepared samples have spinel structure. The particle sizes of the prepared powder were in the range of 10 nm to 20 nm. XPS showed the valences of Mn and Co to be +4 and +2, respectively. Charge–discharge testing of the $MnCo_2O_4$ as the anode for lithium-ion batteries was carried out at 0.2 mA $cm^{-2}$ from 0.0 V to 3.0 V. The first discharge capacity reached 1448 mAh $g^{-1}$, demonstrating the great potential of $MnCo_2O_4$ as anode material in lithium-ion batteries.

**Key words:** Lithium-ion batteries, anode material, $MnCo_2O_4$, hydrothermal reaction

## INTRODUCTION

Carbon materials such as graphite, when used as conventional anode material in lithium-ion batteries (LIBs), can deliver specific capacity of 372 mAh $g^{-1}$ in theory.[1] However, to match the growing demand for LIBs, higher discharge capacity is needed. Meanwhile, renewed interest in transition-metal oxides as potential anode materials for use in lithium-ion batteries started to grow after the year 2000.[2] In this context, many transition-metal oxides with spinel structure[3–8] have been studied and are expected to become promising anode materials in the future; for example, Alcantara et al.[9] obtained $NiFe_2O_4$ powder via precipitation of a mixed oxalate precursor, achieving a first discharge capacity of 1000 mAh $g^{-1}$. Zhao et al.[1] also prepared $NiFe_2O_4$ by hydrothermal method, with initial discharge capacity reaching 1314 mAh $g^{-1}$. Sharma et al.[10] synthesized $MgCo_2O_4$ particles by oxalate decomposition method, with initial discharge capacity of 736 mAh $g^{-1}$. Sharma et al.[11] also obtained $ZnCo_2O_4$ particles via urea combustion method, with initial discharge capacity of 960 mAh $g^{-1}$.

Among these transition-metal oxides, spinel $MnCo_2O_4$ has been studied widely as a magnetic material. However, as an anode material for LIBs, $MnCo_2O_4$ has received little attention. Lavela[12] and his team have focused on the electrochemical properties of $MnCo_2O_4$ particles using the sol–gel method, with initial discharge capacity of 1200 mAh $g^{-1}$. The size of the prepared $MnCo_2O_4$ particles was 80 $\mu$m. This result indicates that $MnCo_2O_4$ could be a promising electrode material for use in lithium-ion batteries. It is well known that nanotechnology can be successfully applied to improve the electrochemical performance of electrode materials.[13,14]

The hydrothermal method is often used to synthesize nanomaterials. Using this route, the size, morphology, and crystal structure of the products are easily controlled. The reaction temperature is also lower.[15] In this work, nanoscale $MnCo_2O_4$ particles were successfully synthesized via hydrothermal method. The electrochemical performance of the as-prepared powder was evaluated.

(Received April 22, 2011; accepted July 21, 2012; published online August 28, 2012)

## EXPERIMENTAL PROCEDURES

$MnCo_2O_4$ nanoparticles were prepared by the hydrothermal method. Typically, 0.8451 g $MnSO_4 \cdot H_2O$, 2.8110 g $CoSO_4 \cdot 7H_2O$, and a little polyglycol were dissolved in 40 ml deionized water. The mixed solution was stirred for 5 h. The pH was maintained at about 10 by adding ammonia solution. The resultant solution was transferred into a Teflon-lined stainless-steel autoclave. The autoclave was kept at 180°C for 8 h, and then air-cooled to room temperature. The resulting precipitate was washed with distilled water several times and finally dried at 120°C.

Powder x-ray diffraction (XRD) analysis using Cu $K_\alpha$ radiation was employed to identify the crystalline phase of the prepared $MnCo_2O_4$ powder with a Bruker D8-Advance (Germany) at room temperature in the range of $10° \le 2\theta \le 70°$. Rietveld analysis was carried out using TOPS R refinement software. X-ray photoelectron spectrometry (XPS) of the reaction products was carried out using an x-ray photoelectron spectrometer (Thermo VGMulti Lab 2000, America). Each spectrum was calibrated using the C 1s binding energy at 284.6 eV. The morphology was investigated by transmission electron microscopy (TEM, FEI, TECNAI G220 S-Twin, America). Simulated cells were assembled by using lithium foil as the cathode in an argon-filled glovebox, the as-prepared powders mixed with 12% acetylene black and 8% polytetrafluoroethylene (PTFE) as the anode, and 1 M $LiPF_6$ in a 1:1 (v/v) mixture of ethylene carbonate (EC) and dimethylcarbonate (DMC) as the electrolyte, with Celgard 2300 membrane as the cell separator. Charge–discharge cycles were performed at 0.2 mA $cm^{-2}$ in the potential range from 3.0 V to 0.0 V using the simulated cells. All electrical measurements were carried out by using a battery testing system (RFT-5 V/10 mA, corporation of LuHua electronic equipment, China) at room temperature. Cyclic voltammograms (CV) were measured with a CHI660A electrochemical workstation (CHI Instruments, TN).

## RESULTS AND DISCUSSION

### XRD Analysis

A typical XRD pattern of an as-synthesized sample is shown in Fig. 1. All the diffraction peaks can be indexed as a pure spinel structure phase of space group *Fd3m* $MnCo_2O_4$ (PDF number: 23-1237). No additional peaks for other phases such as CoO or $MnO_2$ were observed. The cell parameter obtained from Rietveld refinement with a convincing $R_{wp}$ value (1.891%) is $a$ = 8.3151 Å.

### TEM Analysis

Images of the prepared $MnCo_2O_4$ samples were observed by TEM. As seen in Fig. 2, the $MnCo_2O_4$ particles have analogous spherical shape. The sizes range from 10 nm to 20 nm. Some particle aggregation is clearly seen, which might have been caused by the intrinsic magnetic nature of $MnCo_2O_4$.[1] On the other hand, with larger surface area, the surface energy is higher, which easily led to agglomeration. The Fourier transformation of the corresponding selected-area electron diffraction (SAED) pattern is shown in Fig. 2d. The interplanar spacing of 0.25 nm is well matched to the standard $d_{311}$ value (0.2507 nm) of spinel $MnCo_2O_4$.

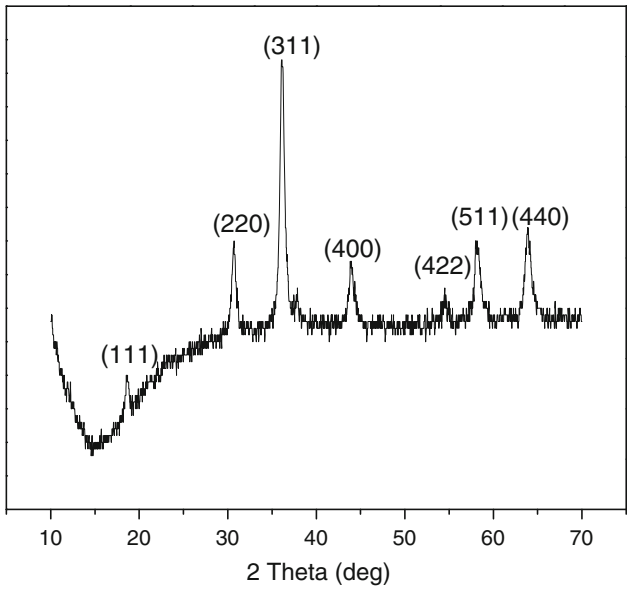


Fig. 1. Typical XRD patterns of the $MnCo_2O_4$ particles.

### XPS Analysis

XPS was used to investigate the composition and valence of the elements of the as-synthesized powder. As seen in Fig. 3, the Co 2p binding energy is 779.21 eV. This is in agreement with $Co^{2+}$ in CoO, which indicates that the valence of Co is +2.[16] The Mn 2p binding energy was located at 641.6 eV. This is in agreement with $Mn^{4+}$ in $MnO_2$, which indicates that the oxide valence of Mn element is +4.[17] Combining this with the XRD results mentioned above, the spinel $MnCo_2O_4$ has been successfully synthesized.

### Electrochemical Performance of $MnCo_2O_4$

The first three charge–discharge curves are shown in Fig. 4. The synthesized $MnCo_2O_4$ nanoparticles were used as the anodic material. The first discharge capacity reached a value of 1448 mAh $g^{-1}$, which is almost four times higher than that of the common carbonaceous materials. During the charge–discharge process, lithium-ion diffusion plays a key role in the capacity.[18] Smaller particle size can shorten the $Li^+$ diffusion distance and increase the capacity. There are two voltage plateaus in the discharge curve. The first one at ~1.4 V is shorter, and the large one at ~0.78 V is followed by a sloping profile to the cutoff voltage of 0 V. The overall discharge capacity is 1448 mAh $g^{-1}$. However, the first charge curve shows

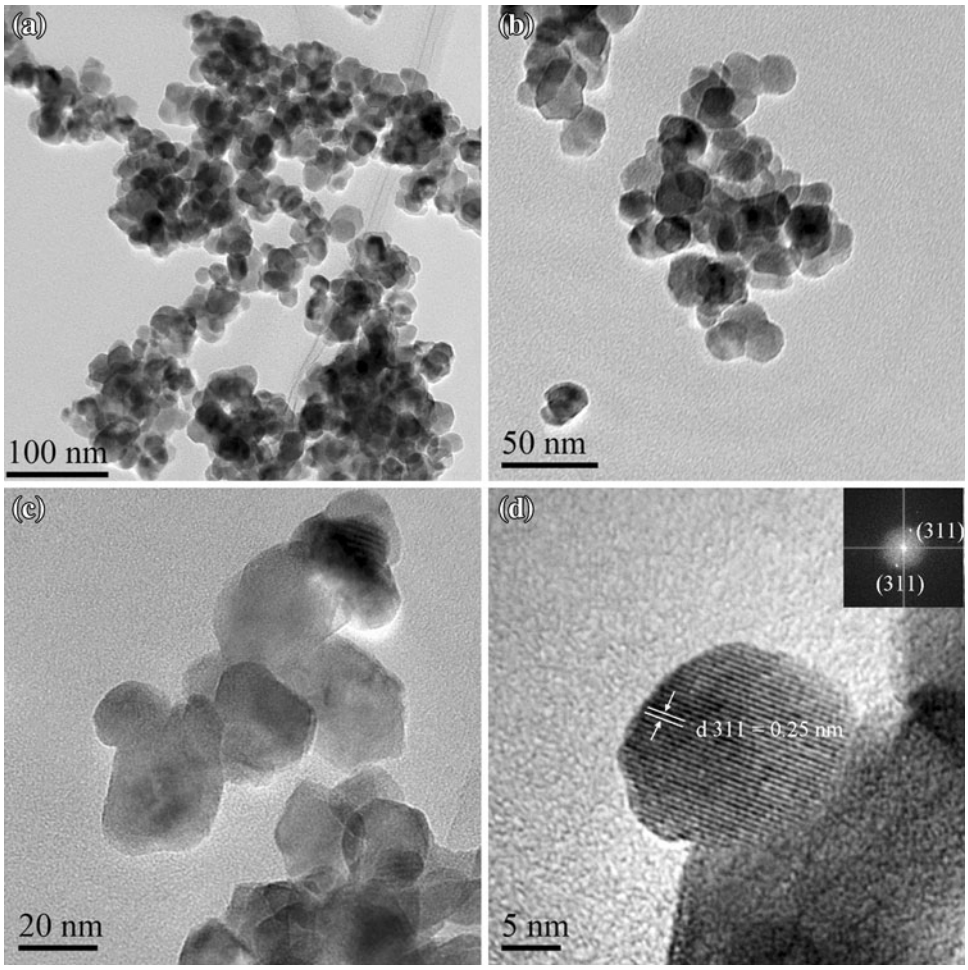


Fig. 2. (a–d) TEM images of $MnCo_2O_4$ nanoparticles, and (d, inset) Fourier transform of the corresponding SAED pattern.

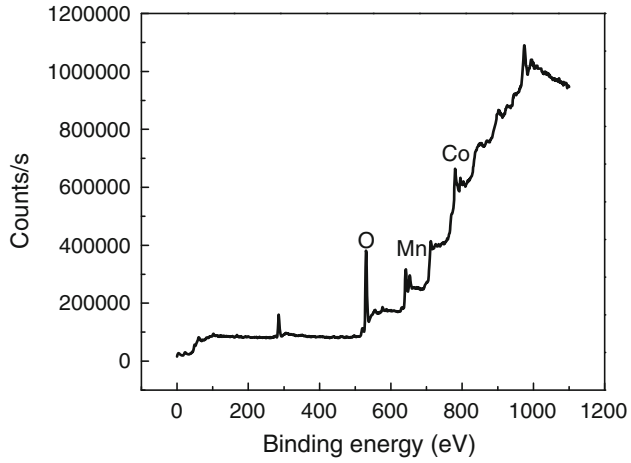


Fig. 3. XPS survey spectrum of $MnCo_2O_4$.

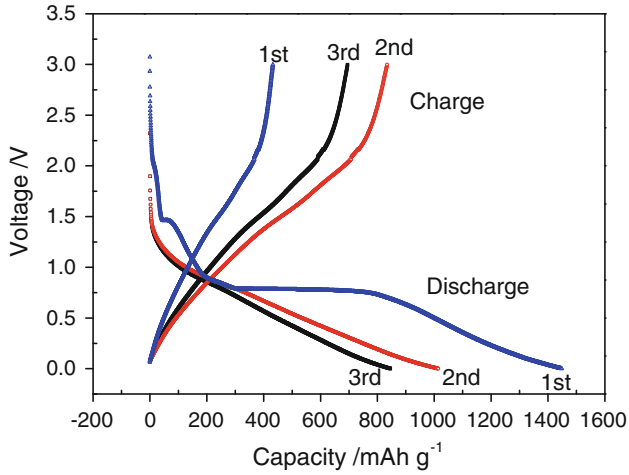


Fig. 4. Initial charge–discharge curve of the $MnCo_2O_4$ nanoparticles at 0.0 V to 3.0 V.

a smoothly varying profile, and the overall charge capacity is 434 mAh $g^{-1}$. The larger irreversible capacity can also be seen in the later cycling, which is the major drawback of these potential candidates for the anode electrode of lithium-ion batteries.[9] It is generally believed that irreversible capacity is related to electrolyte decomposition and the formation of an organic layer on the surface of the particles when the cell potential approaches 0 V.[19] The second and

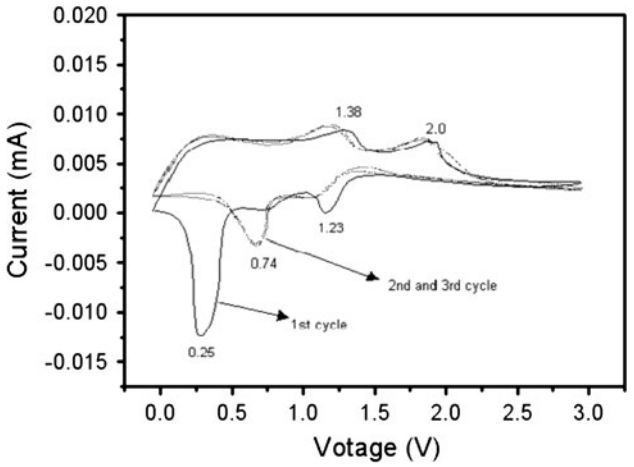


Fig. 5. The first three consecutive CVs of $MnCo_2O_4$ electrode at 0.2 mV $s^{-1}$ from 0.00 V to 3.00 V.

third discharge capacities were 1060 mAh $g^{-1}$ and 870 mAh $g^{-1}$, respectively. Moreover, the charge/discharge capacity ratios were 29.97%, 97.7%, and 98.5% for the first, second, and third cycles, respectively. The coulombic efficiency is obviously improved.

The first three cyclic voltammograms of $MnCo_2O_4$ are shown in Fig. 5. Lithium foil was used as the counterelectrode and reference electrode. The scan rate is 0.2 mV $s^{-1}$, and the potential is in the range of 0.00 V to 3.00 V. The first cycle is substantially different from the subsequent two. According to Ref. 20, the peak centered at 0.23 V can be assigned to reduction of $Mn^{2+}$ and $Co^{2+}$ to metallic Mn and Co in the first cycle, accompanied by decomposition of the organic electrolyte to form a solid electrolyte interphase (SEI) layer. This SEI layer usually forms at the electrode/electrolyte interphase by reduction of electrolyte.[21] The peak at 1.23 V may be attributed to reduction of $Mn^{4+}$ to $Mn^{2+}$. From the second cycle onward, there are two pairs of redox peaks at about 0.74 V/1.38 V and 1.22 V/2.0 V, which might originate from reduction/oxidation of MnO and CoO, respectively.

## CONCLUSIONS

In this work, nanosized $MnCo_2O_4$ was prepared by the hydrothermal route. The XRD data show that the prepared $MnCo_2O_4$ particles have spinel structure. The size of the prepared $MnCo_2O_4$ nanoparticles is in the range of 10 nm to 20 nm. The electrochemical performance of the $MnCo_2O_4$ as anodic material for lithium-ion batteries was tested. The initial discharge capacity reached 1448 mAh $g^{-1}$. Thus, $MnCo_2O_4$ nanoparticles are expected to be a promising anode material for lithium-ion batteries in future applications.

## ACKNOWLEDGEMENTS

This work was supported by the Special Fund for Basic Scientific Research of Central Colleges, South-Central University for Nationalities (CZZ10002).

## REFERENCES

1. H.X. Zhao, Z. Zheng, K.W. Wong, S. Wang, B.J. Huang, and D.P. Li, *Electrochem. Commun.* 9, 2606 (2007).
2. P. Poizot, P.S. Laruelle, S. Grugeon, S.L. Dupont, and J.-M. Tarascon, *Nature* 407, 496 (2000).
3. Y. Sharma, N. Sharma, G.V. Subba Rao, and B.V.R. Chowdari, *Electrochim. Acta* 53, 2380 (2008).
4. R.K. Selvan, N. Kalaiselvi, C.O. Augustin, C.H. Dohb, and C. Sanjeeviraja, *J. Power Sources* 157, 522 (2006).
5. Y.N. Li and Q.Z. Qin, *J. Power Sources* 142, 292 (2005).
6. P. Lavela and J.L. Tirado, *J. Power Sources* 172, 379 (2007).
7. P. Lavela, G.F. Ortiz, J.L. Tirado, E. Zhecheva, R. Stoyanova, and S. Ivanova, *J. Phys. Chem. C* 111, 14238 (2007).
8. Y.Q. Chu, Z.W. Fu, and Q.Z. Qin, *Electrochim. Acta* 49, 4915 (2004).
9. R. Alcantara, M. Jaraba, P. Lavela, J.L. Tirado, J.C. Jumas, and J. Olivier-Fourcade, *Electrochem. Commun.* 5, 16 (2003).
10. Y. Sharma, N. Sharma, G.V. Subba Rao, and B.V.R. Chowdari, *Solid State Ionics* 179, 587 (2008).
11. Y. Sharma, N. Sharma, G.V. Subba Rao, and B.V.R. Chowdari, *Adv. Funct. Mater.* 17, 2855 (2007).
12. P. Lavela, J.L. Tirado, and C. Vidal-Abarca, *Electrochim. Acta* 52, 7986 (2007).
13. L. Gireaud, S. Grugeon, S. Pilard, P. Guenot, J.M. Tarascon, and S. Laruelle, *Anal. Chem.* 78, 3688 (2006).
14. H. liu, L. Tan, and Z. Luo, *J. Alloys Compd.* 502, 407 (2010).
15. T. Mousavand, S. Ohara, M. Umetsu, J. Zhang, S. Takami, T. Naka, and T. Adschiri, *J. Supercrit. Fluids* 40, 397 (2007).
16. H. Qiao, L. Xiao, and L. Zhang, *J. Power Sources* 185, 486 (2008).
17. Y. Li, H. Xie, J. Wang, and L. Chen, *Mater. Lett.* 65, 403 (2011).
18. Y.C. Sun, Y.G. Xia, and H. Noguchib, Electrochem. Solid State Lett. A637 (2005).
19. X.D. Li, W.S. Yang, F. Li, D.G. Evans, and X. Duan, *J. Phys. Chem. Solids* 67, 1286 (2006).
20. L. Zhou, D. Zhao, and X.W. Lou, *Adv. Mater.* 24, 745 (2012).
21. Y. Wang, D.W. Su, A. Ung, J. Ahn, and G.X. Wang, *Nanotechnology* 23, 055402 (2012).